Journal of Materials Science: Materials in Electronics (2019) 30:6544–6551
https://doi.org/10.1007/s10854-019-00960-7

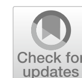

Study on material properties of Sn- and Cu-doped ZnO thin films as n- and p-type thermoelectric materials based on wet solution synthesis

Doanh Viet Vu[1] · Dang Hai Le[1] · Tinh Trong Nguyen[2] · Thiet Van Duong[3] · Quan Duc Ngo[3] · Thong Quang Trinh[3]

Received: 25 November 2018 / Accepted: 16 February 2019 / Published online: 4 March 2019
© Springer Science+Business Media, LLC, part of Springer Nature 2019

Abstract

Sn-doped n-type and Cu-doped p-type ZnO films were fabricated by depositing solutions derrived by sol–gel route on glass substrates through dip-coating cycles. The X-ray diffractometry demonstrates the typical crystalline structure of hexagonal wurzite of ZnO. The surface morphology was made through scanning electronmicroscopy showing the density and shape of films' grains of which size was determined between 40 and 55 µm. The results of Hall measurement indicate clearly the material nature of fabricated films at room temperature. The best electrical property of Sn-doped n-type ZnO films is corresponding to Sn content of 2 at.% with carrier concentration of 3.0×10^{18} cm^{-3}. The formation of p-type ZnO thin films was elucidated by the manner of solution synthesis that glucose was added into the solube mixer of zinc acetate and copper(II) nitrate trihydrate and the way of thermal treatment for films in vacuum with pretty good hole concentration of about 10^{15} cm^{-3}. The electrical transport properties characterizing thermoelectric (TE) behavior of all films were investigated between room temperature to 400 °C (or from 300 to 673 K). The obtained results of electrical conductivity, Seebeck coefficient and power factor revealed that Sn-doped n-type ZnO films have the quality and properties similar to Al-doped ones and Cu-doped ZnO films can be promising p-type materials for TE applications.

1 Introduction

In recent years, the interest in research on thermoelectric (TE) materials for making the devices including generators (TEG) and coolers (TEC) that exploit the waste heat is at a high point because of the trend and necessity to implement the renewable energy. The typical TEGs or TECs employ TE couples of n-type and p-type semiconducting materials connected electrically in series but thermally in parallel. In principle, the good TE materials are ones which produce a large potential difference across the sample when exposed to a temperature gradient. Therefore, they should have high carrier concentration and mobility as well as low thermal conductivity. In this scope, bulk and nano-structured metal chalcogenides which are compounds and alloys based on lead and bismuth in combination with antimony, tellurium and selenium demonstrated their good TE high-performance and become most popular industrial and commercial TE materials during the past years [1–3]. However, there are the issues of cost, thermally unstable and possible toxicity of those materials for the environment in actual applications. Then, nanostructured metal oxide-based TE materials are interested because of their better chemical and thermal stability and small electronic contribution to the thermal conductivity [4, 5].

The nanostructured zinc oxide (ZnO) is a most popular semiconductor which has been studied for a long time due to widely applications for opto-electric devices, sensors particularly recent discovery for the TE modules [6–12]. The advantages of this material are inexpensive, nontoxic and compatible with semiconductor manufacturing processes. ZnO has the nature of the n-type conductivity because its ionicity resides at the borderline between the covalent and ionic semiconductors and the impurities due to native defects [10]. That's why it is convenient to have intensified n-type ZnO by introducing the elements that can release electrons to conduction band by substituting Zn sites. The typical dopants used for this aim are group IIIA elements

✉ Thong Quang Trinh
thong.trinhquang@hust.edu.vn

1 Faculty of Chemistry, Hanoi National University of Education, 136 Xuan Thuy Rd., Hanoi, Vietnam

2 Institute of Applied Physics and Scientific Instruments, Vietnam Academy of Science and Technology, 18 Hoang Quoc Viet Rd., Hanoi, Vietnam

3 School of Engineering Physics, Hanoi University of Science and Technology, 1 Dại Co Viet Rd., Hanoi, Vietnam

such as Al and Ga [9, 13]. On the contrary, modifying electrical behavior of ZnO to have stable p-type material is still a hard work because of unclear mechanism of dopant's substitution in its structure [15, 16]. For this target many studies on successful p-doping using group V including N, As, and Sb have been reported [9, 14, 15]. Generally, finding a suitable acceptor impurity for reliable p-type ZnO remains opened for research [16].

In this context, we report a study of ZnO films doped with Sn of group IVA as n-type material and Cu of group IB as p-type one. The films were fabricated by dipping method using the solutions synthesized by sol–gel method considered a low-cost and simplicity that is appropriate for poor research condition in developing countries. This approach was more encouraged because so far there have been also many relevant reports about the Sn- and Cu-doped ZnO thin films [17–27]. However, all the reported investigations mostly mentioned the applications of the materials for optical devices and gas sensors. Meanwhile, the target of our study is for TE applications. Therefore, there are several different aspects compared to the other researches in the process of solution synthesis and film fabrication for optimizing the electrical and thermal properties of samples. The material characterizations of doped ZnO films such as crystal microstructures, surface morphology, and electrical property showing carrier type, concentration and mobility as well temperature-dependent Seebeck coefficient and power factor were measured and analyzed.

2 Experimental procedures

In this work, the solutions were synthesized by sol–gel reaction using the precursors which are inorganic salts including zinc acetate dihydrate (ZnAc) for forrming ZnO, tin(II) chloride dihydrate ($SnCl_2{\cdot}2H_2O$) as n-dopant source and/or copper(II) nitrate trihydrate ($Cu(NO_3)_2{\cdot}3H_2O$) as p-type one. The chemicals were solved and mixed together in various appropriate molar ratios of precursors to have the desired dopant concentration in a range from 1 to 3 at.% for both of Sn and Cu as presented in Table 1. The reason of light doping concentrations is because a good TE material requires high electrical conductivity but low thermal one that which is also contributed by the charge carrier transport. In our experiments, isopropanol ($CH_3CH(OH)CH_3$) or IPA, 2-methoxyethanol ($CH_3OCH_2CH_2OH$) or 2-ME are used as solve instead of triethylenamin (TEA) as reported in our previous work [28] that can improve the zinc precursor solubility and to stabilize the starting solutions. Ethylene glycol ($C_2H_4(OH)_2$) or EG is additive. Particularly, for case of cooper doping, glucose ($C_6H1_2O_6$) was utilized for the reduced reaction making the transition Cu^{2+} to Cu^{1+} ions with the molar number as that of copper(II) nitrate trihydrate. In the scenario, the mol number of glucose used equals that of copper(II) nitrate trihydrate. The doped ZnO films were made by dipping the glass substrate (Corning 1737F) on synthesized solutions with rate of 20 mm per minute for several times in combination with prebaked process at 250 °C for each immersion to dry and remove the residual solvents. The films were annealed at 550 °C for 4 h for structural crystallization. In this procedure, Sn-doped ZnO (SZO) films were thermally treated in the environment of N_2 but in vacuum for Cu-doped ZnO (CZO) ones.

The structural characteristics of the deposited ZnO films were investigated by X-ray diffraction (XRD) (Cu–Kα, Siemen D5005 Brucker, λ = 1.54056 A) with the 2θ scanning range from 20° to 70°. The surface morphology of the films was observed using a scanning electron microscopy (SEM) system of Hitachi HR-S4800 that also allows determining the thickness and grain size of deposited films. The basic electrical properties at room temperature were measured by using the Hall-effect system of Lake Shore 8400 Series. Lastly, the electrical transports characterizing for TE property of fabricated films were investigated by using a home-made measurement setup.

3 Results and discussion

Figure 1 is the result of microstructure analysis of ZnO film samples doped with different concentrations of Sn and Cu in comparison to ZnO one. It reveals that the fabricated films are all well-crystallized with a hexagonal wurtzite structure (Zincite, JCPDS 36-1451) [29] considered the most stable structure of ZnO. Namely, all film peaks are corresponding to the specific planes including (002) planes at around

Table 1 Calculated mixing ratio among precursors for synthesis of sol–gel solutions

Chemical	$Zn(CH_3COOH)_2{\cdot}2H_2O$		$SnCl_2{\cdot}2H_2O$		$Cu(NO_3)_2{\cdot}3H_2O$	
Doping concentration (%)	Molar number	Weight (g)	Molar number	Weight (g)	Molar number	Weight (g)
1	0.015	3.2925	0.000152	0.0342	0.000152	0.0367
2	0.015	3.2925	0.000306	0.0692	0.000306	0.0741
3	0.015	3.2925	0.000464	0.1048	0.000464	0.1123

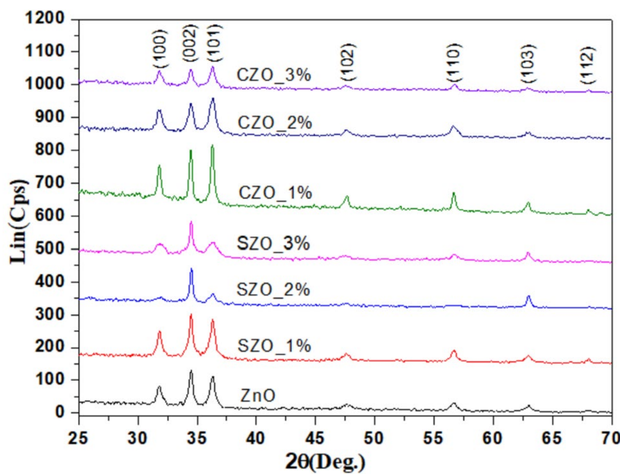

Fig. 1 XRD patterns of undoped and doped ZnO thin films with different Sn and Cu doping content

34.5°, (100) and (101) at around 31.8° and 36.2°. The presence of those prominent peaks confirms the polycrystalline in nature. There are no any additional phases of Sn, Cu and the oxides of those metals like spinels of tetragonal observed in this measurement. All doped ZnO films show a slight shift at (002) peak in comparison with undoped ones. For SZO films, the intensities of diffraction peaks declined as Sn concentrations increased. It means Sn doping within ZnO films caused the crystallinity to degenerate that can be considered an evidence for the replacement of Sn^{+4} ions at Zn^{+2} sites. The increase in doping percentage leads to the strong (002) peak intensities exhibiting c-axis preferred orientation. Possibly the Sn^{+4} ions are smaller radii than Zn^{2+} ions leading to the decrease in grain size of doped films. As a result, the grain boundaries increase enhancing the phonon scatterings considered an expected result for TE property. Nevertheless, the result of microstructure analysis also proclaims that (002) plane is not really preferential orientation for CZO films. It is worth noting that the intensity of all the diffraction peaks decreases for all the orientations with the Cu content increasing, suggesting the films crystallinity worsening with Cu doping at a certain degree. This may be caused by the change in nucleation centers from being homogenous to heterogeneous [30]. In addition, all peaks tend to shift towards the higher angles when increasing the Cu content that leads to a decrease in c parameter lattice compared to bare ZnO samples. The tendency can also make the decrease in grain size of ZnO films with larger mol concentration of Cu dopant. It is because for Cu doping, not only Cu^{+2} ions but also Cu^{+1} ones can replace either substitution or interstitial Zn atoms in the ZnO lattice that can make structural deformations. In general, the obtained XRD spectra for CZO films in our study are pretty similar to those in the reported works [20]. Based on the XRD patterns, the average grain sizes estimated using Scherrer's equation [31] for both of two types of films are in range of 40 to 50 nm.

The SEM images of films morphology showing the shape and grain density that can provide the insight of their microstructure and allow affirming the results of XRD patterns mentioned above. Figure 2 shows the results for bare ZnO films as well as SZO (Fig. 2a) and CZO (Fig. 2b) ones with doping concentrations from 1 to 3% mol. For the convenience of comparison, all images are in the same scale of 500 nm. In general, all films fabricated based on wet route process have moderate smooth surface when annealed at 550 °C. The SZO films have the increased density with increasing dopant's content. The quality of SZO films are also better than that of CZO ones because there are no pores. Viewing from the surface, the grain sizes of both types of films are gradually decreased with increasing doping concentrations. Possibly, the cause is the incorporation of the dopants into the host material leading to the increasing number of nucleation and the disturbance of grain growth by stress due to the difference in ionic radius of dopants and zinc. However, this result is expected for TE performance because the decreased grain sizes lead to the increase in the grain boundaries that will increase phonon scattering for minimizing the thermal conductivity of material. Visually, the grains are in hexagonal shape for bare ZnO and SZO samples. For CZO films, owing to the preferential orientation shown in XRD pattern and two possible substitutes of Cu ions in ZnO structure, it may result in the wormlike form of grains of CZO films. Fortunately, what we can see from SEM images are in relatively good agreement with the structure analyses of XRD spectra. From SEM results the average grain sizes of two types of doped ZnO films were determined in a range of 45 to 55 nm. In addition, the thickness of films was also examined by using this measurement. Based on the optimized dipping process, all fabricated films are pretty uniform with the thickness in range from 250 to 265 nm as illustrated in Fig. 3 for two typical samples. The cross-sectional images also supplement obviously the film density that can be seen in the surface SEM ones. The EDX technique was also implemented for checking the ratio of Sn and Cu element in the samples. The analysis results are pointed out in Fig. 4 for cases of ZnO films doped with 2 at.% Sn and Cu. The peaks characterizing for all elements of doped ZnO films as well as those of glass substrate can be easily observed in the spectra. The concentration of two dopants was found to be relatively close to the expected one. Namely, it is corresponding to 2.14 at.% for Sn and 2.04 at.% for Cu.

The basic electrical parameters of bare and doped ZnO films including resistivity, carrier mobility and concentration received from Hall measurement is shown in Fig. 5. In our work, the resistivity of all films derived from sol–gel solutions are relatively high compared to the others fabricated

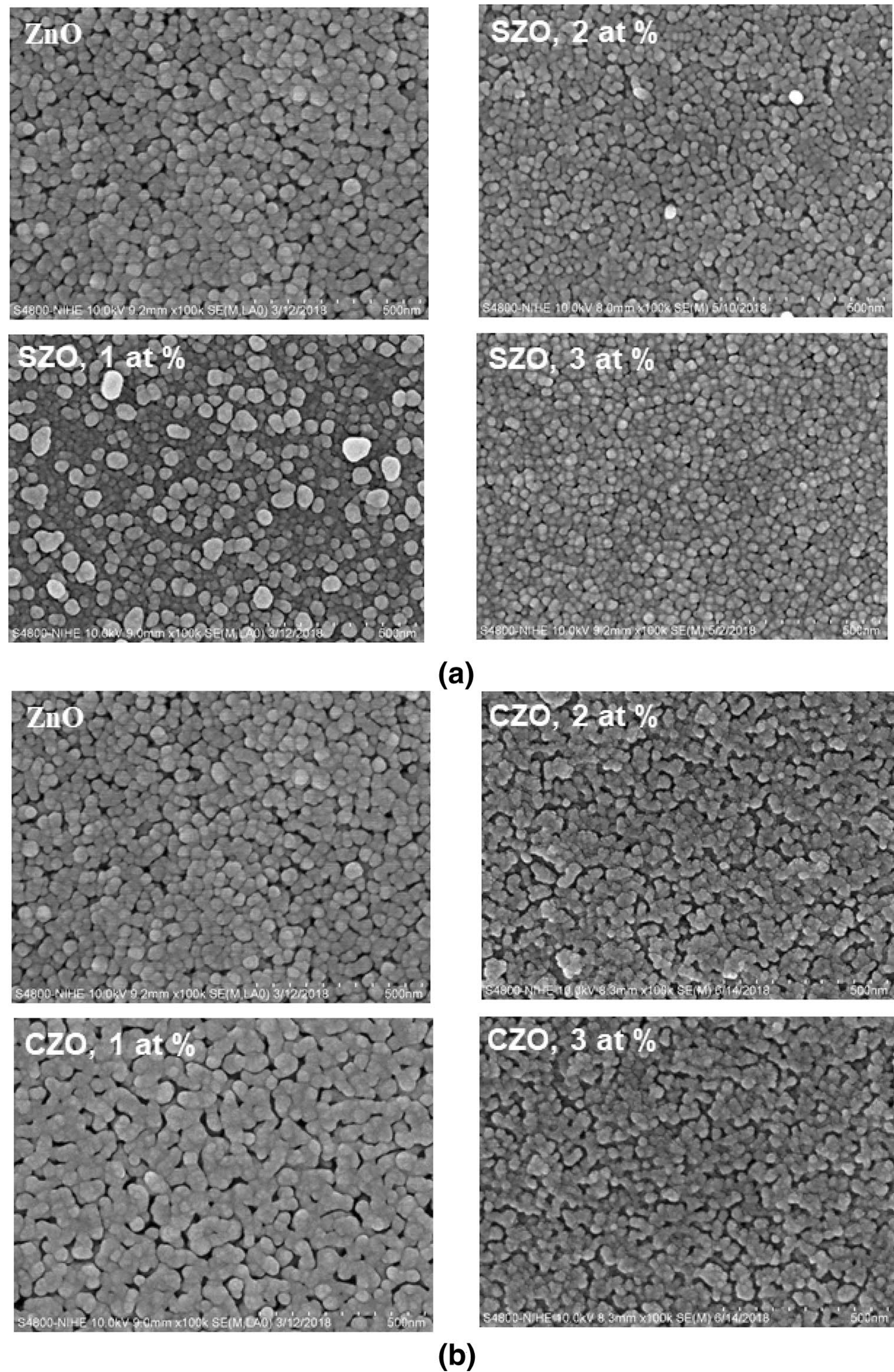

Fig. 2 SEM surface micrographs of undoped and doped ZnO thin films

by vapor vacuum methods but also similar to the reported investigations based on the same approach [17, 27, 32]. In case of n-type SZO samples, the incorporation of Sn^{4+} ions at Zn^{2+} sites could behave as a doubly ionized donor leading to the increase in carrier concentration of SZO with increasing the doping amount. For this type of films, the best values of resistivity, carrier mobility and concentration are 28.3 Ωcm, 20.5 $cm^2/V\,s$ and 3.0×10^{18} cm^{-3}, just corresponding to the dopant content of 2 at.% while those parameters of bare ZnO films are 480 Ωcm, 3.9 $cm^2/V\,s$, and 2×10^{15} cm^{-3}, respectively. In this situation, perhaps, the more dopants lead to the tendency that tin atoms occupy the interstitial sites where they form neutral defects. As a result, the resistivity increased but both carrier mobility and

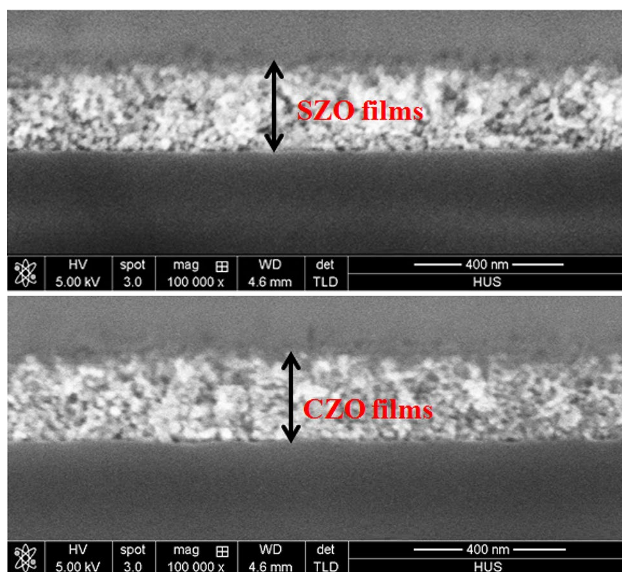

Fig. 3 SEM cross-sectional images of SZO and CZO films

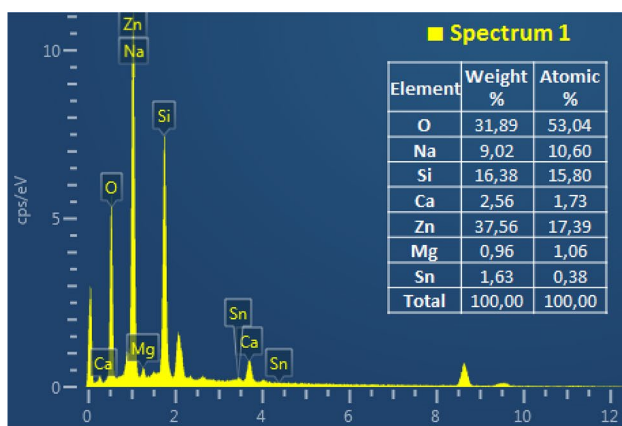

Element	Weight %	Atomic %
O	31,89	53,04
Na	9,02	10,60
Si	16,38	15,80
Ca	2,56	1,73
Zn	37,56	17,39
Mg	0,96	1,06
Sn	1,63	0,38
Total	100,00	100,00

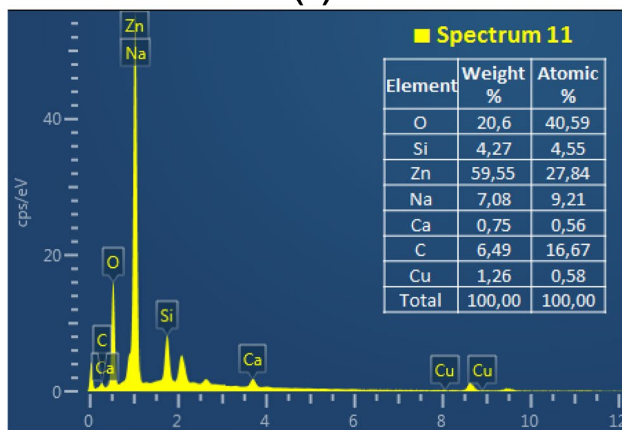

Element	Weight %	Atomic %
O	20,6	40,59
Si	4,27	4,55
Zn	59,55	27,84
Na	7,08	9,21
Ca	0,75	0,56
C	6,49	16,67
Cu	1,26	0,58
Total	100,00	100,00

Fig. 4 EDX spectra of ZnO films doped with 2 at.% Sn (**a**) and 2 at.% Cu (**b**)

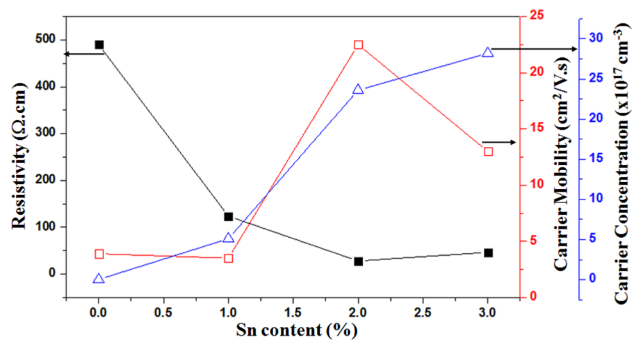

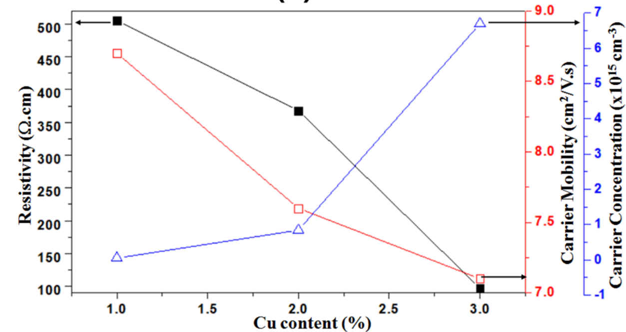

Fig. 5 Electrical property of Sn-doped n-type (**a**) and Cu-doped p-type (**b**) ZnO thin films at room temperature

concentration decreased. Most measurement results for CZO samples reveal the film material is p-type semiconductor with positive Hall coefficient. It is well-known that both Cu^{1+} and Cu^{2+} atoms can coexist in ZnO. When the Cu^{2+} ions outnumber they have a tendency to form deep donor levels, resulting in n-type nature of material [33, 34]. However, it has been proven that the Cu^{1+} ions can trap free electrons with Cu 3d hole state to create a shallow acceptor level above the valence band therefore they are responsible for p-type conductivity. In our procedure of solution synthesis, glucose was also used that the reduced reaction happened resulting in the transition of Cu^{2+} to Cu^{1+} ions. Additionally, the Cu-doped ZnO samples were thermally annealed in vacuum that also support the process of Cu^{2+} ions to be reduced to Cu^{1+} contributing to the increase in number of Cu^{1+} ions, as suggested by previous works [32, 35–38]. The average hole concentrations approximately equal to 5.5×10^{12} cm^{-3}, 8.4×10^{14} cm^{-3}, and 6.7×10^{15} cm^{-3} for CZO films with corresponding cooper content of 1, 2, 3 at.%, respectively. From the obtained results, it suggests that more Cu contents may be introduced into the ZnO lattice to increase more carrier concentration.

The electrical transport properties and TE characterizations including electrical conductivity, Seebeck coefficient, and power factor of doped ZnO thin films were investigated in range of room temperature up to 400 °C (673 K). Figure 6

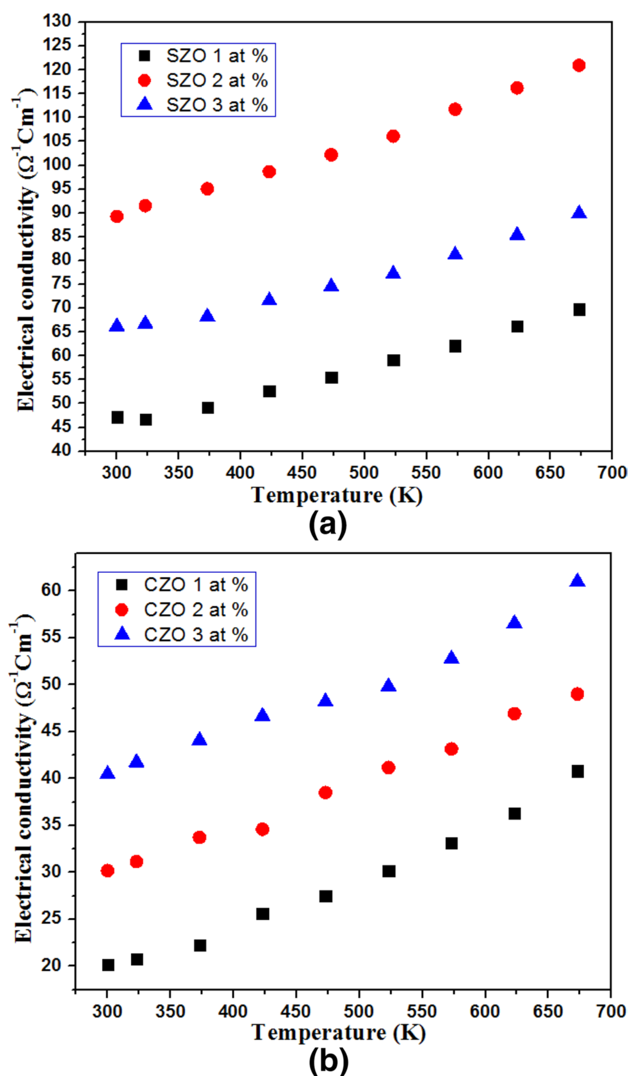

Fig. 6 Temperature dependence of electrical conductivity Sn-doped n-type (**a**) and Cu-doped p-type (**b**) ZnO thin films

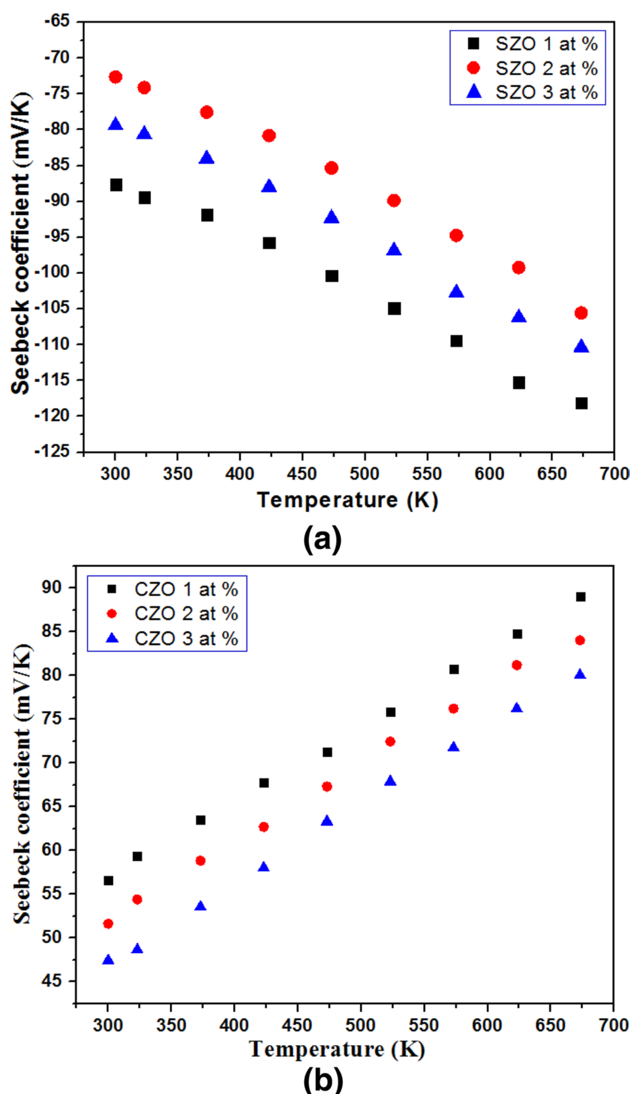

Fig. 7 Seebeck coefficient of Sn-doped n-type (**a**) and Cu-doped p-type (**b**) ZnO thin films

demonstrates the electrical conductivity of both types of doped films relying on the measurement of sheet resistance by using four-probe method. This property increases with temperature (in K) showing the semiconductor behavior of materials. As can be seen in the graphs, the electrical conductivities of n-type samples are greater than those of p-type ones because resistivity of Sn-doped ZnO films is smaller than that of Cu-doped films. The best electrical conductivity for Sn-doped films is corresponding to Sn content of 2 at.% and it is 3 at.% for Cu-doped ZnO ones. The measurement results for Seebeck coefficient of all samples are shown in Fig. 7. As expected, this characterization confirms the materials nature such that the Seebeck coefficients for Sn-doped samples have negative values as n-type materials but positive for Cu-doped films as p-type ones. In general, for both film cases, the Seebeck coefficients increase with temperature showing totally the semiconductor's behavior. The worst values of Seebeck coefficient of SZO films are for samples that have the best electrical conductivity corresponding to 2 at.%. It is because better electrical conductivity tends to make rapidly the balance of temperatures between two ends of measurement due to the thermal conductivity of electrons. However, the Seebeck coefficients of CZO films increase with the increasing of doped Cu content. It is also attributed by the low formation energy of Cu for substitution, the defect band with small effective mass formed inside and the narrow band gap of ZnO that is considered good for improving the transport properties with increased Cu content.

Finally, the power factors (*PF*) characterizing for the performance of the TE energy converter were calculated based on the Seebeck coefficient and electrical conductivity as indicated in Fig. 8. There is a similar trend of Seebeck coefficient

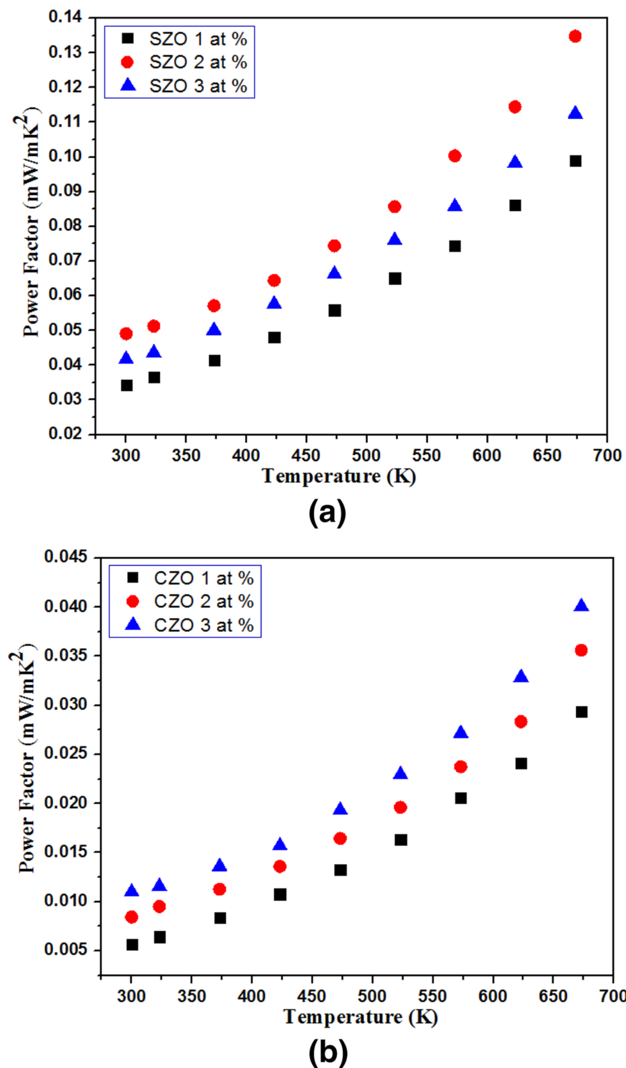

Fig. 8 Power factor of Sn-doped n-type (**a**) and Cu-doped p-type (**b**) ZnO thin films

characteristics that the values increase with the measuring temperatures (in K). It can be seen that the SZO films show the relatively good efficiency of thermoelectricty. Namely, the best value of pF for this type of films is about 0.14 mW/mK^2 for sample with 2 at.% which can be compared to Al-doped films reported in our previous work [28]. The values of PF for CZO films are small compared to n-type samples doped with Sn. It is because the electrical properties of CZO films are not as good as those of SZO ones.

4 Conclusion

In this work, a study of Sn and Cu-doped ZnO thin films deposited by sol–gel dip coating technique as n-type and p-type TE materials were implemented. A doping range for both Sn and Cu contents is in range from 1 to 3 at.%. As revealed by XRD measurements both types of doped films have wurtzite crystal structure and their preferential crystallographic orientation can be modified by increasing the dopant concentration. The introduce of dopants affected the grain sizes and shapes resulting in the increase in the grain boundary. The EDX spectra confirmed that the dopant concentrations are present in the fabricated films as expected. The electrical properties of all films were investigated by a combination of measurements of Hall effect, Seebeck effect and sheet resistance. The SZO films were successfully prepared showing good improvement in the electrical property, especially for the sample having Sn content of 2 at.% that can be compared with typical TE Al-doped ZnO ones. Obvious p-type behavior was observed for Cu-doped ZnO films with promising electrical properties among which the hole concentration reaches 10^{15} cm^{-3}. The p-type behavior was attributed by the increasing the number of Cu^+ ions through the use of glucose in synthesis process and thermal treatment in vacuum. Although the stability of Cu-doped p-type ZnO films remains an issue, our experimental results indicate that CZO films could be an alternative candidate for TE applications.

Acknowledgements This work has been supported by the Vietnam's National Foundation for Science and Technology Development (NAFOSTED) grant funded by Ministry of Science and Technology (MOST) under (Grant No. 103.02-2017.304).

References

1. V.S. Zemskov, L.E. Shelimova, P.P. Konstantinov, E.S. Avilov, M.A. Kretova, I.Yu. Nikhezina, Inorg. Mater. Appl. Res. **3**, 61–68 (2012)
2. A. Powell, P. Vaqueiro, in *Thermoelectric Materials and Devices, RSC Energy & Environment Series*, ed. by I. Nandhakumar, N.M. White, S. Beeby (Royal Society of Chemistry, London, 2016), pp. 27–59
3. S. Li, X. Li, Z. Ren, Q. Zhang, J. Mater. Chem. A **6**, 2432–2448 (2018)
4. W.J. Fergus, J. Eur. Ceram. Soc. **32**, 525–540 (2012)
5. S. Hébert, A. Maignan, *Thermoelectric Oxides* (Wiley, Hoboken, 2010), pp. 203–255
6. Ü Özgür, Ya.I. Alivov, C. Liu, A. Teke, M.A. Reshchikov et al., J. Appl. Phys. **98**, 041301 (2005)
7. V.A. Coleman, C. Jagadish, in *Zinc Oxide Bulk, Thin Films and Nanostructures*, ed. by C. Jagadish, S. Pearton, (Elsevier, New York, 2006), pp. 1–20
8. P. Uikey, K. Vishwakarma, Int. J. Emerg. Techol. Comput. Sci. Elec. **21**, 239–242 (2016)
9. A. Janotti, C.G. Van de Walle, Rep. Prog. Phys. **72**, 126501 (2009)
10. A. Mahmood, A. Naeem, in *Recent Applications in Sol–Gel Synthesis*, ed. by C. Usha, (Intech, London, 2017), pp. 169–193
11. Y. Wang, C. Zhou, A.M. Elquist, A. Ghods, V.G. Saravade, N. Lu, I. Ferguson, A review of earth abundant ZnO-based materials for thermoelectric and photovoltaic applications, in Proceedings of the Oxide-based Materials and Devices, (SPIE, San Francisco, 2018). https://doi.org/10.1117/12.2302467

12. M.A. Mohammed, I. Sudin, A.M. Noor, S. Rajoo, M.B. Uday, N.H. Obayes, M.F. Omar, Int. J. Eng. Techol. **2**, 6649–6655 (2018)
13. C.D. Look, *Doping and Defects in ZnO, in Thin Films and Nanostructures*, ed. by C. Jagadish, S. Pearton, (Elsevier, New York, 2006), pp. 21–42
14. F. Xiu, J. Xu, P.C. Joshi, A.C. Bridges, M.P. Paranthaman, Springer Ser. Mater. Sci. **218**, 105–140 (2016)
15. J.C. Fan, K.M. Sreekanth, Z. Xie, S.L. Chang, K.V. Rao, Prog. Mater. Sci. **58**, 874–985 (2013)
16. C.H. Park, S.B. Zhang, S.H. Wei, Phys. Rev. B **66**, 073202 (2002)
17. C.-Y. Tsay, H.-C. Cheng, Y.-T. Tung, W.-H. Tuan, C.-K. Lin, Thin Films Solid **517**, 1032–1036 (2008)
18. K.J. Chen, F.Y. Hung, Y.T. Chen, S.J. Chang, Z.S. Hu, Mater. Trans. **51**, 1340–1345 (2010)
19. M. Vishwas, K. Narasimha Rao, K.V. Arjuna Gowda, R.P.S. Chakradhar, Spectrochim. Acta **95**, 423–426 (2012)
20. N.H. Hashim, S. Subramani, M. Devarajan, A.R. Ibrahim, J. Mater. Sci. Mater. Electron. **27**, 3520–3530 (2014)
21. M.F. Nasir, M.N. Zaino, M. Hannas, M.H. Mamat, S.A. Rahman, AIP Conf. Proc. (2015). https://doi.org/10.1063/1.4948885
22. D. Wang, J. Zhou, G. Liu, J. Alloys Compd. **487**, 545–549 (2009)
23. K. Chongsri, S. Aunpang, W. Techitdheera, W. Pecharapa, Adv. Mater. Res. **802**, 124–128 (2013)
24. T. Saidani, M. Zaabat, M.S. Aida, A. Benaboud, S. Benzitouni, A. Boudine, Superlattices Microstruct. **75**, 47–53 (2014)
25. H. Gómez-Pozos, E.J.L. Arredondo, A.M. Álvarez, et al., Materials (2016). https://doi.org/10.3390/ma9020087
26. S. Horzum, E. Torun, T. Serin, F.M. Peeters, Philos. Mag. **96**, 1743–1756 (2016)
27. C. Boukaous, S. Ghanem, A. Teli, B. Benhaoua, Mater. Res. Express **4**, 105024 (2017)
28. T.Q. Trinh, T.T. Nguyen, D.V. Vu, D.H. Le. J. Mater. Sci. Mater. Electron. **28**, 236–240 (2017)
29. H.F. Mc Murdie, M.C. Morris, E.H. Evans, B. Paretzkin, W. Wong-Ng, L. Ettlinger, C.R. Hubbard, *JCPDS Research Associateship*, vol. 1 (Cambridge University, Cambridge, 1986), pp. 64–77
30. M. Öztas, M. Bedir, Thin Solid Films **516**, 1703–1709 (2008)
31. B.D. Cullity, S.R. Stock, *Elements of X-ray Diffraction*, 3rd edn. (Prentice Hall Inc, Saddle River, 2001), pp. 167–171
32. A. Hartmann, M.K. Puchert, R.N. Lamb, Surf. Interface Anal. **24**, 671–674 (1996)
33. M.B. Rahmani, S.H. Keshmiri, M. Shafiei, K. Latham, W. Wlodarski, Sens. Lett. **7**, 1–8 (2009)
34. S.Y. Lee, N. Mettlach, N. Ngugen, Y.M. Sun, J.M. White, Appl. Surf. Sci. **206**, 102–109 (2003)
35. Y. Yanfa, M.M. Al-Jassim, S.H. Wei, Appl. Phys. Lett. **89**, 1819121–1819123 (2006)
36. J.-B. Lee, H.-J. Lee, S.-H. Seo, J.-S. Park, Thin Solid Film **398**, 641–646 (2004)
37. M. Suja, S.B. Bashar, M.M. Morshed, J. Liu, ACS Appl. Mater. Interfaces **7**, 8894–8899 (2015)
38. K. Yim, J. Lee et al., Sci. Rep. **7**, 40907 (2017)

Publisher's Note Springer Nature remains neutral with regard to jurisdictional claims in published maps and institutional affiliations.